

## Research Article

# An Efficient Blind Image Deblurring Using a Smoothing Function

Kittiya Khongkraphan , Aniruth Phonon , and Sainuddeen Nuiphom 

Faculty of Science and Technology, Prince of Songkla University, Pattani 94000, Thailand

Correspondence should be addressed to Kittiya Khongkraphan; [kittiya.k@psu.ac.th](mailto:kittiya.k@psu.ac.th)

Received 3 November 2020; Revised 19 March 2021; Accepted 30 March 2021; Published 17 April 2021

Academic Editor: Isidoros Perikos

Copyright © 2021 Kittiya Khongkraphan et al. This is an open access article distributed under the Creative Commons Attribution License, which permits unrestricted use, distribution, and reproduction in any medium, provided the original work is properly cited.

This paper introduces an efficient deblurring image method based on a convolution-based and an iterative concept. Our method does not require specific conditions on images, so it can be widely applied for unspecific generic images. The kernel estimation is firstly performed and then will be used to estimate a latent image in each iteration. The final deblurred image is obtained from the convolution of the blurred image with the final estimated kernel. However, image deblurring is an ill-posed problem due to the nonuniqueness of solutions. Therefore, we propose a smoothing function, unlike previous approaches that applied piecewise functions on estimating a latent image. In our approach, we employ  $L_2$ -regularization on intensity and gradient prior to converging to a solution of the deblurring problem. Moreover, our work is based on the quadratic splitting method. It guarantees that each subproblem has a closed-form solution. Various experiments on synthesized and real-world images confirm that our approach outperforms several existing methods, especially on the images corrupted by noises. Moreover, our method gives more reasonable and more natural deblurred images than those of other methods.

## 1. Introduction

An image deblurring is a recovering process that recovers a sharp latent image from a blurred image, which is caused by camera shake or object motion. It has widely attracted attention in image processing and computer vision fields. A number of algorithms have been proposed to address the image deblurring problem. The most common approaches to blur removal are to treat blur as a noisy convolution operated with a blur kernel. The mathematical form of the blurred image is then usually modelled as

$$y = x * k + n, \quad (1)$$

where  $y$  is a blurred image,  $x$  is a corresponding latent image,  $k$  and  $n$  denote the blur kernel and white noise, respectively, and  $*$  represents the convolution operator.

A number of approaches have been proposed to address deblurring image problem, and one of popular approaches was based on the deconvolution-based concept. There are two types of approaches: nonblind and blind deconvolutions. The main difference between these two types is that the blur kernel must be known as prior in the case of nonblind

deconvolution. The blur kernel estimation is an essentially important step in obtaining a high-quality sharp image. Most approaches use statistical priors on natural images and selection of salient edges for the blur kernel estimation [1–6]. Moreover, several researchers estimate a high-quality blur kernel directly from the input image with motion blur by studying the problem in the frequency domain [7–9].

In the blind deconvolution, the goal is to estimate both the corresponding latent image and the blur kernel. The blind deconvolution is an ill-posed problem since it has many pairs of solutions. To deal with the blind deblurring problem well-posed, most blind image deblurring methods tend to formulate the problem as a minimization problem. The blur kernel and the latent image are usually solved in an alternating fashion. The algorithm will converge quickly if an appropriately useful initialization is well chosen. However, various assumptions or regularizations are demanded. Pan et al.[10] presented  $L_0$ -regularized intensity and gradient prior to deblurring text images. This method is suitable for text images with a clean background, but it is less useful for a cluttered background. Liu et al.[11] combined  $L_0$ -regularized of both first- and second-order image gradients in order to

standardize the final estimation results. Cho et al. [12] developed a method to incorporate text-specific properties for deblurring. This prior outperformed in two-tone images; however, it is still less effective in generic images.

Many researchers proposed numerous image-priors underlining optimization techniques to resolve the ill-posed problem in generic images. Pan et al. [13] continued to propose their work with the generic images via modifying a dark channel firstly introduced by He et al. [14]. It is based on the observation that, in most of the natural scene patches, at least one of the color channels possesses some pixels with very close to zero intensities. This algorithm enforces the sparsity of the dark channel of latent images for kernel estimation and generates better results compared to other approaches. However, the dark channel may not help intermediate latent image estimation if there are no dark pixels in the images, but instead, there is a large degree of bright pixels.

Yan et al. [15] proposed a novel natural image prior named Extreme Channels Prior (ECP) by taking the advantages of both Dark Channel Prior (DCP) and Bright Channel Prior (BCP) to refine natural images. This method is more robust and performs favourably against the state-of-the-art image deblurring methods on both synthesized and natural images. However, it has limitations and is less likely to support kernel estimation. The kernel estimation process is complicated, and the performance depends mainly on the intensity values of images. Several researchers turned to employ a gradient prior to improve the accuracy of kernel estimation. Shan et al. [16] adopted a sparse image prior and introduced a unified probabilistic model to fit the gradient distribution of natural images to solve the kernel estimation problems. The authors in [17, 18] proposed a hyper-Laplacian prior to fit the distribution of natural image gradients for avoiding local solutions. Fergus et al. [1] presented an algorithm using a zero-mean mixture of Gaussians to learn the image gradient prior to fitting the distribution of natural image gradients. Zhong et al. [19] proposed an adaptive generalized variation (TGV) regularized model to remove deblurring and maintaining fine image details.

All proposed algorithms [3–15] added the auxiliary terms in objective functions. Based on the observation, we found that the closed forms of auxiliary terms are in terms of the piecewise functions containing the parameters. These parameter values were constantly updated by scaling, leading to the loss of detail in the images. Moreover, most algorithms require specific conditions on generic images so they cannot be widely applied for nonspecific generic images.

In this paper, we present an efficient optimization algorithm based on the quadratic splitting method. The splitting method guarantees that each subproblem has a closed-form solution and ensures fast convergence. Additionally, we introduce a novel smoothing function for updating pixel values and a sigmoid function for scaling parameters. Our smoothing function based on  $L_2$ -regularized intensity and gradient prior gives a significant advantage result and can reduce the loss of details in the images. Moreover, our approach is also suitable for colored images that do not require any specific conditions on the image.

This paper is organized as follows. Our  $L_2$ -regularization method is described in Section 2. Section 3 describes our blind image deblurring method. In Section 4, we present some experimental results. Finally, conclusions are drawn in Section 5.

## 2. Our $L_2$ -Regularization Method

We first formulate the blind image deblurring to a minimization problem and introduce a new efficient regularization term for convergence to a solution of deblurring. As we mentioned, equation (1) is solvable. That is,  $E(y) = \{(x, k) | y = x * k + n\}$  is not empty. We seek an  $x$  corresponding with a kernel  $k$  whose norm is the minimum. However, we first need to confirm that such a solution always exists in the set  $E(y)$ . Given a latent image  $x$  and a blur kernel  $k$ , a blurred image  $y$  can be rewritten as  $KX$ , where  $K$  is the Toeplitz matrix and  $X$  is the column latent image  $x$ . So, we have  $y = KX$ . To show that  $y = KX$  has the solution with the minimum norm, we need the following proposition.

**Proposition 1.** *Let  $W$  and  $Z$  be Hilbert space,  $G \in L(W, Z)$  and  $G^* \in L(Z, W)$  the adjoint operator; then the following statement holds:*

$$\text{Rang}(G) = Z \text{ if and only if there exists } \gamma > 0 \text{ such that } \|G^*z\|_W \geq \gamma \|z\|_Z, z \in Z$$

$$\overline{\text{Rang}(G)} = Z \text{ if and only if } G^* \text{ is one to one}$$

Now, the matrix  $K$  may be viewed as a linear operator  $K: \mathbb{R}^m \rightarrow \mathbb{R}^n$ ; therefore,  $K \in L(\mathbb{R}^m, \mathbb{R}^n)$ . Since  $y = KX$  is solvable for all  $y$ ,  $K$  is surjective. Hence, by Proposition 1, there exists  $\gamma > 0$  such that  $\|K^*z\| \geq \gamma \|z\|, z \in \mathbb{R}^n$ .

Therefore,  $\langle KK^*z, z \rangle \geq \gamma^2 \|z\|_2^2, z \in \mathbb{R}^n$ . This implies that  $KK^*$  is one to one. Hence,  $\det(KK^*) \neq 0$ . We can see that  $X = K^*(KK^*)^{-1}y$  is a solution of  $y = Kz$ . Now, we shall see that this solution has a minimum norm. In fact, consider  $W \in \mathbb{R}^m$  such that  $KW = y$  and

$$\|W\|_2^2 = \|X + (W - X)\|_2^2 = \|X\|_2^2 + \|W - X\|_2^2 + 2\text{Re} \langle X, W - X \rangle. \quad (2)$$

Note that

$$\begin{aligned} \langle X, W - X \rangle &= \langle K^*(KK^*)^{-1}b, W - X \rangle \\ &= \langle (KK^*)^{-1}b, KW - KX \rangle \\ &= \langle (KK^*)^{-1}b, y - y \rangle = 0. \end{aligned} \quad (3)$$

Hence,  $\|W\|_2^2 - \|X\|_2^2 = \|W - X\|_2^2 \geq 0$ . Therefore,  $\|W\|_2^2 \geq \|X\|_2^2$ . This means that  $X$  has the minimum norm. Therefore, we can conclude that, for every blurred image, there always exists a corresponding latent image  $x$  with a kernel  $k$  whose norm of  $x$  is the minimum. Based on this fact, we confidently believe that seeking out such a latent image with the minimum norm is one of the alternative ways to solve the problem. Thus, we define  $P(x) = \alpha \|x\|_2^2 + \|\nabla x\|_2^2$  as a regularization term in our approach.

### 3. Our Image Deblurring Method

Our image deblurring method is an iterative approach based on a convolution-based concept. In each iteration, the kernel estimation is performed, and then it is used to estimate a latent image. The estimated latent image is then to be as input in the next kernel estimation. The final deblurred image is obtained from a convolution of the blurred image with the final estimated kernel. A system overview of our proposed method is shown in Figure 1.

To estimate the kernel and the latent image, equation (1) is formed as an optimization problem with a regularization term  $P(x)$  for image deblurring expressed as follows:

$$\min_{x,k} \|x * k - y\|_2^2 + \gamma \|k\|_2^2 + \lambda P(x). \quad (4)$$

A solution directly from intensity values is often inaccurate [2, 4, 10], so we set the regularization term in an intensity space and a gradient space with  $P(x) = \alpha \|x\|_2^2 + \|\nabla x\|_2^2$ .

We use an efficient alternating minimization method [2, 5, 10, 13] to solve equation (4). These two subproblems are solved as follows:

$$\min_x \|x * k - y\|_2^2 + \lambda(\alpha \|x\|_2^2 + \|\nabla x\|_2^2), \quad (5)$$

$$\min_k \|x * k - y\|_2^2 + \gamma \|k\|_2^2. \quad (6)$$

The details of the two subproblems are described in the following sections.

**3.1. Estimating the Latent Image  $x$  with the Blur Kernel  $k$ .** We introduce an efficient alternating minimization method to solve equation (5). Like [10, 13, 20], we propose the auxiliary variables  $g = (g_h, g_v)^T$  corresponding to  $x$  and  $\nabla x$ , respectively. The objective function then can be rewritten as

$$\min_{x,u,g} \|x * k - y\|_2^2 + \beta \|x - u\|_2^2 + \mu \|\nabla x - g\|_2^2 + \lambda(\alpha \|u\|_2^2 + \|g\|_2^2), \quad (7)$$

where the constants  $\beta$  and  $\mu$  are weights based on the latent image value and the constants  $\lambda$  and  $\alpha$  are weight values.

To solve equation (7), the values of  $u$  and  $g$  are initialized to be zero in the first iteration. And then, the solution of  $x$  is obtained in each iteration by solving

$$\min_x \|x * k - y\|_2^2 + \beta \|x - u\|_2^2 + \mu \|\nabla x - g\|_2^2. \quad (8)$$

Based on a least square minimization problem, we perform *FFTs* and the closed-form solution is given by

$$x = \mathcal{F}^{-1} \left( \frac{\overline{\mathcal{F}(k)} \mathcal{F}(y) + \beta \overline{\mathcal{F}(u)} + \mu \overline{\mathcal{F}(\nabla)} \mathcal{F}(g)}{\overline{\mathcal{F}(k)} \mathcal{F}(k) + \beta + \mu \overline{\mathcal{F}(\nabla)} \mathcal{F}(\nabla)} \right), \quad (9)$$

where  $\mathcal{F}(\cdot)$  and  $\mathcal{F}^{-1}(\cdot)$  denote the Fast Fourier Transform (*FFT*) and inverse *FFT*, respectively.  $\overline{\mathcal{F}(\cdot)}$  is the complex

conjugate operator.  $\nabla = \nabla_h + \nabla_v$ , where  $\nabla_h$  and  $\nabla_v$  are the horizontal and vertical differential operators, respectively.

To update the variable  $x$ , we first need to compute  $u$  and  $g$ , which can be done separately by

$$\min_u \beta \|x - u\|_2^2 + \lambda \alpha \|u\|_2^2, \quad (10)$$

$$\min_g \mu \|\nabla x - g\|_2^2 + \lambda \|g\|_2^2. \quad (11)$$

Note that equations (10) and (11) are pixel-wise minimization problems, and most importantly, they are smooth. Thus, the solutions of  $u$  and  $g$  are obtained by the simple technique of differentiation:

$$u = \frac{\beta}{\beta + \lambda \alpha} x, \quad (12)$$

$$g = \frac{\mu}{\mu + \lambda} \nabla x. \quad (13)$$

It is worthwhile to note that, in each iteration, the weighted values of  $\beta$  and  $\mu$  are always updated. In most algorithms [3–15], the weighted values of  $\beta$  and  $\mu$  are glued in  $u$  and  $g$ , but in the forms of piecewise function and they are always updated by scaling. This may force values for some pixels to be zero which will lead to the loss of the details in latent images. In fact, we confidently believe that each pixel should not be scaled by the same value but it should depend on itself. So, in our approach, we employ the sigmoid functions  $\beta(x)$  and  $\mu(x)$  for updating the value  $\beta$  and  $\mu$ , respectively, where  $\beta(x) = \lambda \sigma e^{x-a}$  and  $\mu(x) = \lambda e^{x-b}$ , where  $a$  and  $b$  are defined as the center of the transition area. Due to the smoothness of equations (12) and (13), not only does it have less artifact effect, but also it guarantees not losing details in intermediate latent images.

**3.2. Estimating the Blur Kernel  $k$  with the Latent Image  $x$ .** To estimate  $k$ , we employ the latent image  $x$  and the blurred image  $y$  in the gradient space as shown in equation (14) and then apply *FFTs* to solve the least square minimization problem

$$\min_k \|\nabla x * k - \nabla y\|_2^2 + \gamma \|k\|_2^2. \quad (14)$$

The closed form of  $k$  kernel estimation with the latent image  $x$  and the blurred image  $y$  is

$$k = \mathcal{F}^{-1} \left( \frac{\overline{\mathcal{F}(x)} \mathcal{F}(\nabla y)}{f(\nabla x) \mathcal{F}(\nabla x) + \gamma} \right). \quad (15)$$

The proposed method, similar to the state-of-the-art methods, is used as a coarse-to-fine processing strategy for handling the blur kernel estimation. The algorithm is typically efficiently implemented using an image pyramid [2, 10]. The summarization of the main step for the latent image and the blur kernel estimation on one pyramid level is presented in Algorithm 1.

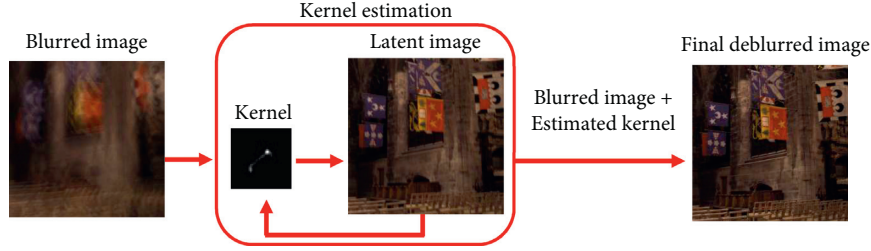


FIGURE 1: System overview of our proposed method.

```

Input: Blur image  $y$ ;
initialize  $k$  with results from the coarser level;
for  $i \leftarrow 1$  to 5 do
   $x \leftarrow y$ ;
   $\beta \leftarrow 2\lambda\alpha$ ;
  repeat
    solve for  $u$  using eq.12;
     $\mu \leftarrow 2\lambda$ ;
    repeat
      solve for  $g$  using eq. 13;
      solve for  $x$  using eq.9;
       $\mu \leftarrow 2\mu$ ;
    until  $\mu > \mu_{\max}$ ;
     $\beta \leftarrow 2\beta$ ;
  until  $\beta > \beta_{\max}$ ;
  solve for  $k$  using eq.15;
   $\lambda \leftarrow \max\{\lambda/1.1, 1e^{-4}\}$ 
end
Output: the latent image and blur kernel

```

ALGORITHM 1: Latent image and blur kernel estimation algorithm.

**3.3. Final Image Restoration.** In the final step, we restore the final deblurred image using nonblind deconvolution, given the final kernel from equation (15). The final latent image can be restored from

$$x = \mathcal{F}^{-1} \left( \frac{\mathcal{F}(k)\mathcal{F}(y) + \mu\overline{\mathcal{F}(\nabla)}\mathcal{F}(g)}{f(k)\mathcal{F}(k) + \mu\overline{\mathcal{F}(\nabla)}\mathcal{F}(\nabla)} \right). \quad (16)$$

We then compute a difference map between these two estimated images with different sigmoid parameters. Finally, we subtract the restored image with a difference map to suppress a ringing artifact.

## 4. Experimental Results

To evaluate the performance of our proposed method, we tested our approach on the real-image datasets [21], synthesized images, and specific domain images [14]. Moreover, we also evaluate the robustness of our approach to Gaussian noise. In all experiments, we set  $\lambda = \sigma = 0.001$  and  $\mu_{\max} = 1e^3, \beta_{\max} = 2^3$ .

**4.1. Evaluation on the Real-Image Datasets.** First, we tested our approach on the image deblurring dataset [21], containing 48 images (4 images with 12 blur kernels). This

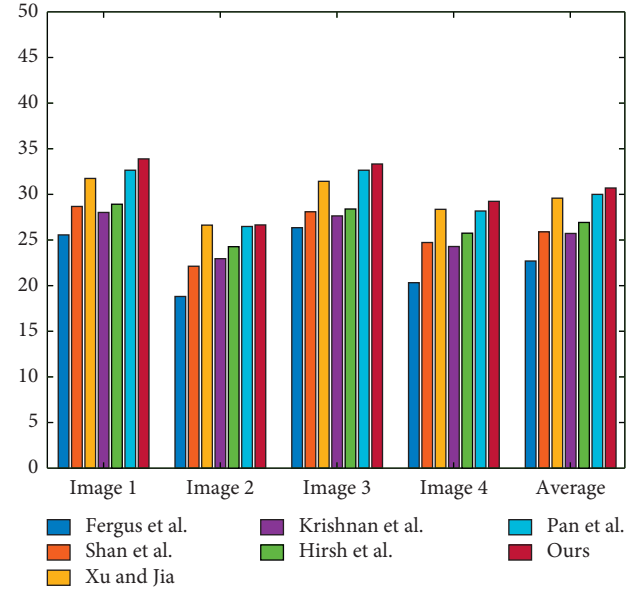


FIGURE 2: Quantitative evaluations on Kohler et al.'s dataset [21].

dataset is used as a benchmark for performance measuring of image deblurring methods. The proposed method is compared with state-of-the-art methods: Cho and Lee [2], Fergus et al. [1], Hirsch et al. [22], Krishnan et al. [23], Whyte et al. [24], Xu and Jia [3], and Pan et al. [13]. To compare performance, we use peak signal-to-noise ratio (PSNR) value which is computed by comparing each restored image with 199 ground truth images. PSNR = 100, which corresponds to a perfect deblurring. The PSNR of our proposed method and those of compared methods on the dataset [21] are illustrated in Figure 2. We found that the PSNR of our approach, Xu and Jia [3], and Pan et al. [13] are not much different in image 2. It might be that on image 2 the balance of the dark and bright pixels is moderately the same. However, our approach gives a higher average PSNR than that of other approaches. Figure 3 shows sample images which are deblurred by the best three algorithms. However, our method gives clearer details and is more natural than that of other approaches.

**4.2. Evaluation on the Synthesized Images.** We then evaluated our approach on the synthesized images with blur kernel. The comparison of results on the first synthesized blurred image is

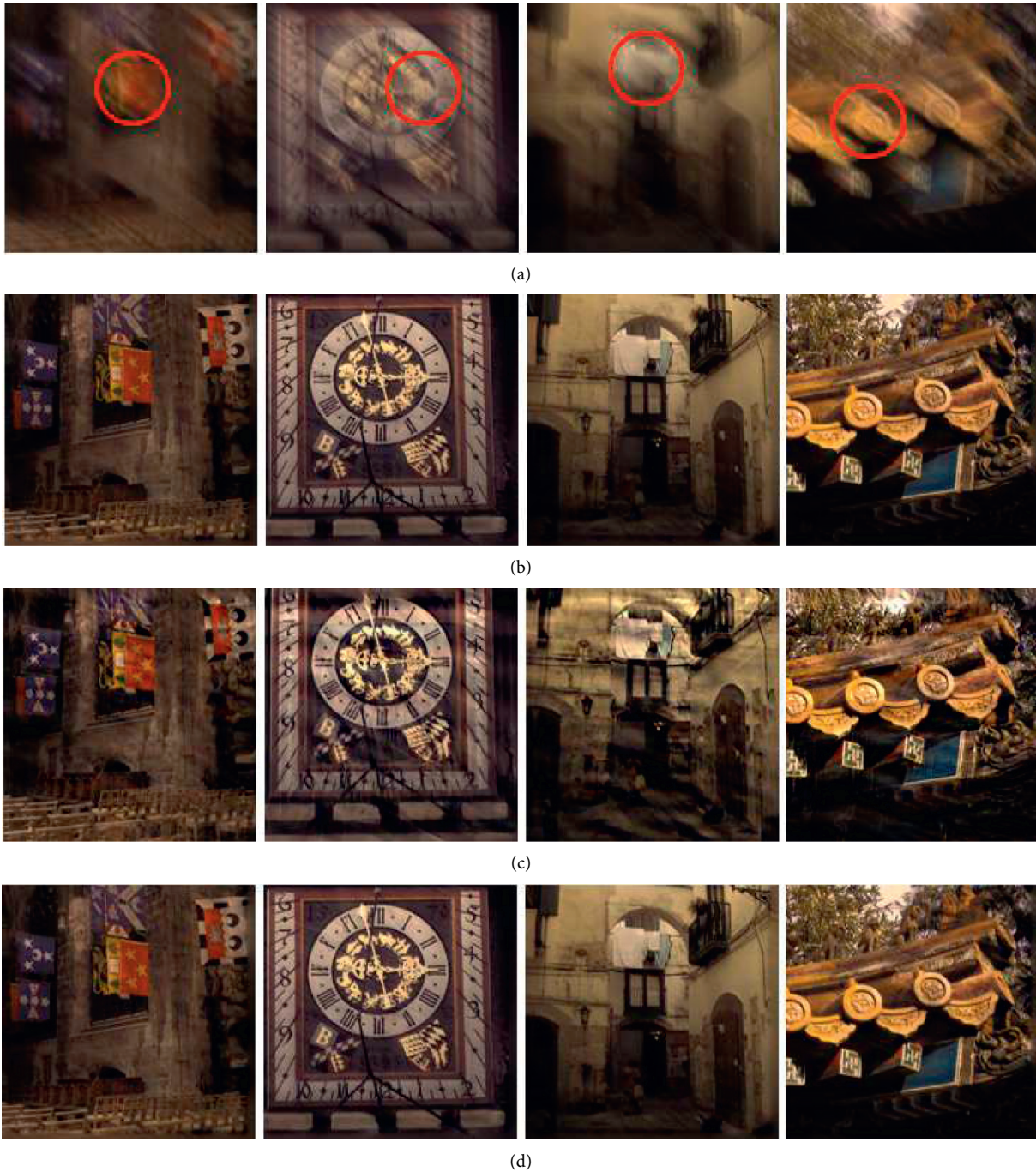


FIGURE 3: Samples of restored image by the best three algorithms on [21]. (a) Blurred image [21]. (b) Xu and Jia [3]. (c) Pan et al. [13]. (d) Ours.

shown in Figure 4. It can be seen that the restored image of our approach gives a better result and is more reasonable than that of other methods. The results from [3, 13] methods redeem more blur than the original image. It might be the case that the original image contains lots of bright pixels. So the two methods could not control the regularization term, which leads to an unreasonable solution.

Moreover, we demonstrated the performance of the proposed method on synthesized blurred images corrupted

by different realizations of the white Gaussian noises, 5–30 *dB*. The samples of synthesized noise blurred images and deblurred images are shown in Figure 5.

The PSNR values for the synthesized images corrupted by various white Gaussian noise levels are shown in Figure 6. Our method achieved the highest PSNR value. It is evident that our method shows outperformance. Our method obviously performs better than the other two methods when the test image contains lots of noise.



FIGURE 4: Comparison of results using a synthesized blurred image. (a) Blurred image. (b) Xu and Jia [3]. (c) Pan et al. [13]. (d) Ours.

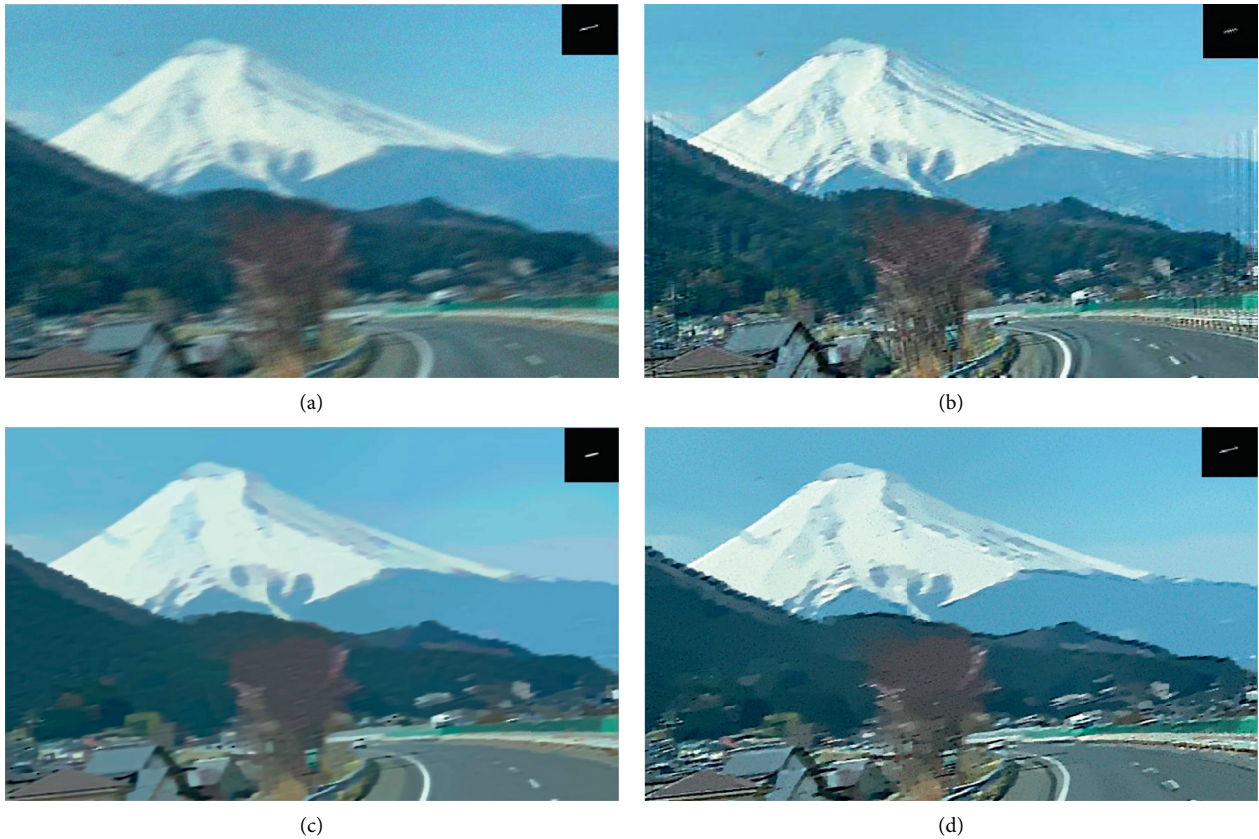


FIGURE 5: Comparison of results using a synthesized blurred image corrupted by noise 30 dB and deblurred images. (a) Blurred image. (b) Xu and Jia [3]. (c) Pan et al. [13]. (d) Ours.

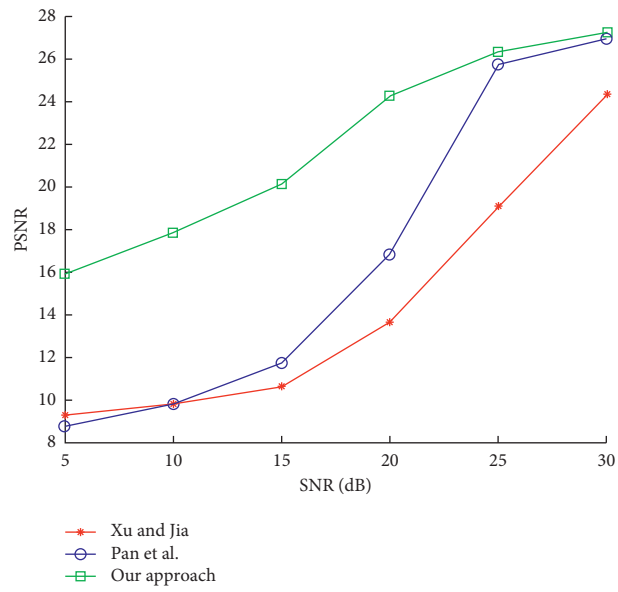


FIGURE 6: The PSNR values of restore images on the synthesized blurred image, corrupted by white Gaussian noises.



FIGURE 7: Comparison of results using a face image. (a) Blurred image. (b) Xu and Jia [3]. (c) Pan et al. [13]. (d) Ours.

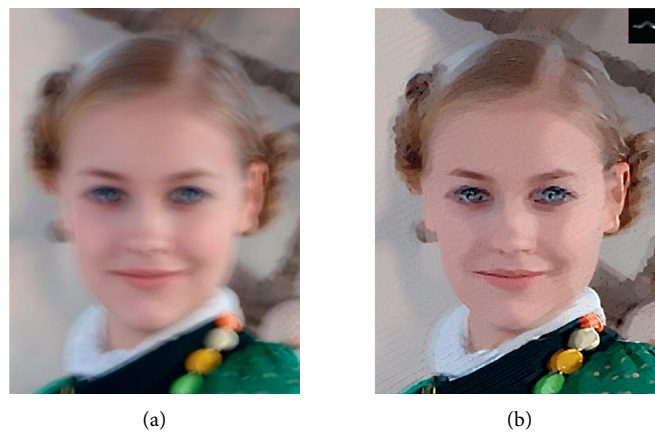


FIGURE 8: Continued.

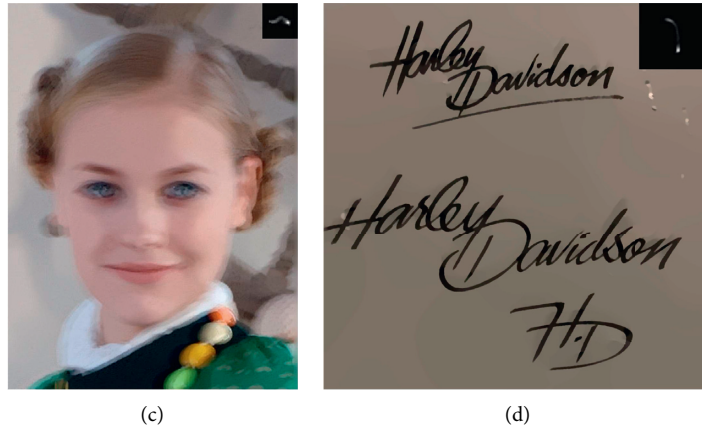


FIGURE 8: Comparison of results using a face image. (a) Blurred image. (b) Xu and Jia [3]. (c) Pan et al. [13]. (d) Ours.

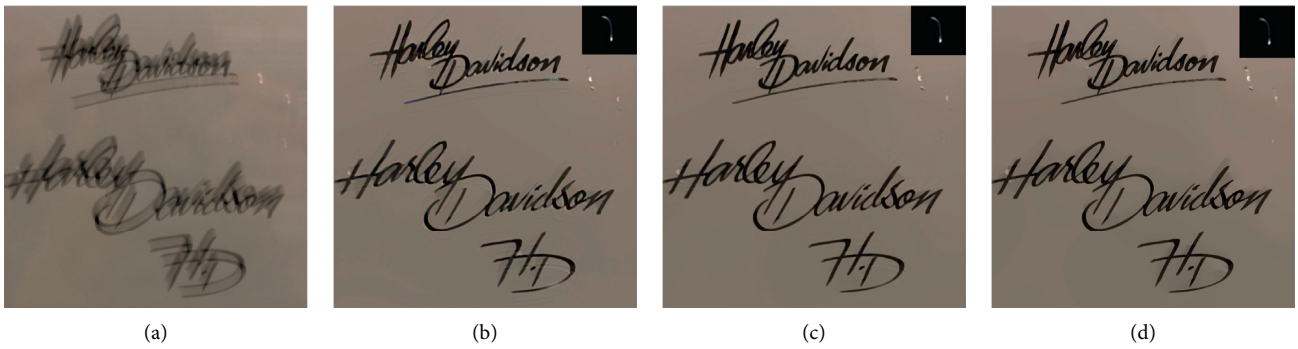


FIGURE 9: Comparison of results using a text image [10]. (a) Blurred image. (b) Pan et al. [10]. (c) Yan et al. [25]. (d) Ours.

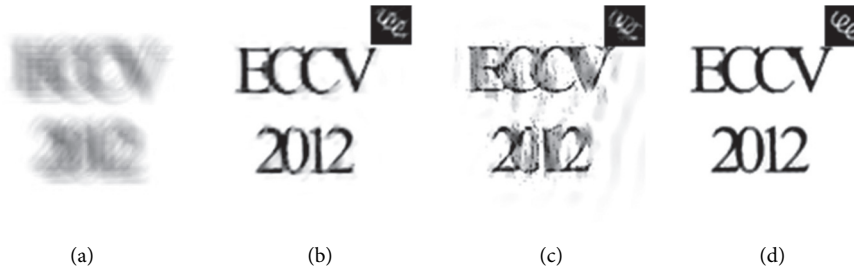


FIGURE 10: Comparison of results using a text image [10]. Evaluation on the robustness to Gaussian noise. (a) Blurred image. (b) Pan et al. [10]. (c) Yan et al. [25]. (d) Ours.



FIGURE 11: Continued.

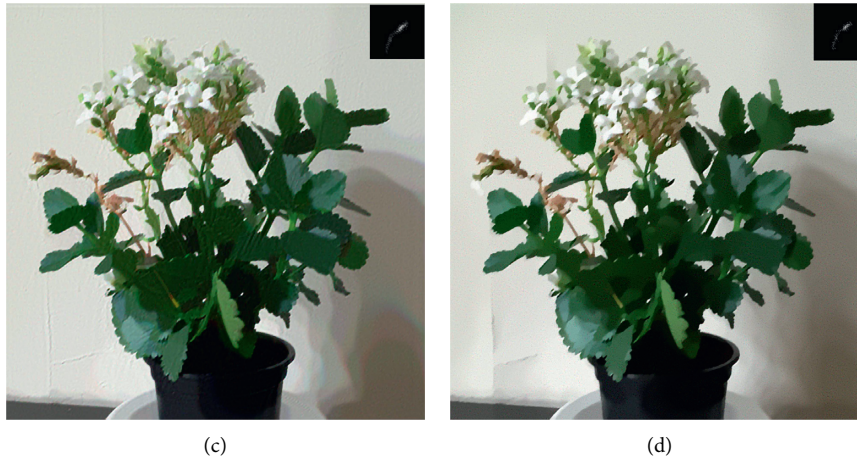


FIGURE 11: Comparison of results on a blurred image with Gaussian noises [14]. (a) Blurred image. (b) Xu and Jia [3]. (c) Pan et al. [13]. (d) Ours.

**4.3. Evaluation on the Specific Domain Images.** The next step, we evaluated the proposed method on the specific domain images such as face and text images. We compared with the advanced deblurring methods in each domain. We then evaluated our approach on face images against the method of Pan et al. [13] that used a dark channel in image deblurring. Moreover, we compared our proposed method to Xu and Jia [3]. As shown in Figures 7 and 8, our method gives more details and is more natural than other methods.

Next, we evaluated the proposed method on selected real and challenging text image for qualitative evaluation as shown in Figures 9 and 10. We compared our method with the methods of Pan et al. [10] and Yan et al. [25] that present specific methods for deblurring the text image. As shown in Figures 9 and 10, our method gives more reasonable, sharper, and less losing details than those of both methods.

We evaluated the robustness of our approach to the blurred image with Gaussian noise. The comparison of results on a blurred image with Gaussian noise is shown in Figure 11. The other methods still contain blur in deblurring results, while ours is more reasonable and more natural. The method of [3] gives more artifacts than other methods. The one in [13] gives an unreasonable result since the noise changed the minimum intensity value of an image patch.

## 5. Conclusions

We propose a novel method for the deblurring image, especially for blind deconvolution. We present  $L_2$  regularization in the deblurring image formed as an optimization problem. This method does not require specific conditions on images, so it can be widely applied for unspecific generic images. It applies smooth functions on estimating a latent image in each iteration. It keeps more details in the restored image than that of existing approaches. To evaluate the performance of our approach, we performed experiments on both synthesized and real-world images. We discovered that our approach outperforms the previous approaches, especially in the image, which contains Gaussian noise. Moreover, our restored

images give more details and are more natural than the restored images produced by other methods.

## Data Availability

Data are available at <https://sites.google.com/site/jspanhomepage/>.

## Conflicts of Interest

The authors declare that they have no conflicts of interest.

## Acknowledgments

This work was supported by the Pattani Campus Research Fund (SAT63030065) from Prince of Songkla University in Thailand.

## References

- [1] R. Fergus, B. Singh, A. Hertzmann, S. T. Roweis, and W. T. Freeman, "Removing camera shake from a single photograph," *ACM Transactions on Graphics*, vol. 25, no. 3, pp. 787–794, 2006.
- [2] S. Cho and S. Lee, "Fast motion deblurring," *ACM Transactions on Graphics*, vol. 28, no. 5, pp. 145–152, 2009.
- [3] L. Xu and J. Jia, "Two-phase kernel estimation for robust motion deblurring," in *Proceedings of the European Conference on Computer Vision*, pp. 157–170, Heraklion, Crete, Greece, September 2010.
- [4] A. Levin, Y. Weiss, F. Durand, and W. T. Freeman, "Efficient marginal likelihood optimization in blind deconvolution," in *Proceeding of the IEEE Conference on Computer Vision and Pattern Recognition*, pp. 2657–2664, Colorado, CO, USA, June 2011.
- [5] L. Xu, S. Zheng, and J. Jia, "Unnatural  $L_0$  sparse representation for natural image deblurring," in *Proceedings of the IEEE Conference on Computer Vision and Pattern Recognition*, pp. 1107–1114, Portland, OR, USA, June 2013.
- [6] J. Pan and Z. Su, "Fast  $L_0$ -regularized kernel estimation for robust motion deblurring," *IEEE Signal Processing Letters*, vol. 20, no. 9, pp. 841–844, 2013.

- [7] R. Dash and B. Majhi, "Motion blur parameters estimation for image restoration," *Optik*, vol. 125, no. 5, pp. 1634–1640, 2014.
- [8] Z. Wang, Z. Yao, and Q. Wang, "Improved scheme of estimating motion blur parameters for image restoration," *Digital Signal Processing*, vol. 65, no. 1, pp. 11–18, 2017.
- [9] L. Pan, R. Hartley, M. Liu, and Y. Dai, "Phase-only image based kernel estimation for single-image blind deblurring," in *Proceedings of the IEEE Conference on Computer Vision and Pattern Recognition*, pp. 6027–6036, Long Beach, CA, USA, June 2019.
- [10] J. Pan, Z. Hu, Z. Su, and M. Yang, "Deblurring text images via L0-regularized intensity and gradient," prior," in *Proceedings of the IEEE Conference on Computer Vision and Pattern Recognition*, pp. 2901–2908, Columbus, OH, USA, September 2014.
- [11] R. W. Liu, W. Yin, S. Xiang, and S. Peng, "L0-regularized hybrid gradient sparsity priors for robust single-image blind deblurring," in *Proceedings of the IEEE Int. Conference Acoustics, Speech Signal Process. (ICASSP)*, pp. 1348–1352, Seoul, Korea, April 2018.
- [12] H. Cho, J. Wang, and S. Lee, "Text image deblurring using text-specific properties," in *Proceedings of the European Conference on Computer Vision*, pp. 524–537, Florence, Italy, October 2012.
- [13] J. Pan, D. Sun, H. Pfister, and M.-H. Yang, "Deblurring images via dark channel prior," *IEEE Transactions on Pattern Analysis and Machine Intelligence*, vol. 40, no. 10, pp. 2315–2328, 2018.
- [14] K. He, J. Sun, and X. Tang, "Single image haze removal using dark channel prior," *IEEE Transactions on Pattern Analysis and Machine Intelligence*, vol. 33, no. 12, pp. 2341–2353, 2011.
- [15] Y. Yan, W. Ren, Y. Guo, R. Wang, and X. Cao, "Image deblurring via extreme channels prior," in *Proceedings of the IEEE Conference on Computer Vision and Pattern Recognition*, pp. 6978–6986, Honolulu, HI, USA, July 2017.
- [16] Q. Shan, J. Jia, and A. Agarwala, "High-quality motion deblurring from a single image," *ACM Transactions on Graphics*, vol. 27, no. 3, pp. 1–10, 2008.
- [17] A. Levin, Y. Weiss, F. Durand, and W. T. Freeman, "Understanding and evaluating blind deconvolution algorithms," in *Proceedings IEEE Conference on Computer Vision and Pattern Recognition*, pp. 1964–1971, Miami, Florida, March 2009.
- [18] Y. Lou, A. L. Bertozzi, and S. Soatto, "Direct sparse deblurring," *Journal of Mathematical Imaging and Vision*, vol. 39, no. 1, pp. 1–12, 2011.
- [19] Q. Zhong, C. Wu, Q. Shu, and R. W. Liu, "Spatially adaptive total generalized variation-regularized image deblurring with impulse noise," *Journal of Electronic Imaging*, vol. 27, no. 05, p. 1, 2018.
- [20] J. Tang, X. Shu, G.-J. Qi et al., "Tri-clustered tensor completion for social-aware image tag refinement," *IEEE Transactions on Pattern Analysis and Machine Intelligence*, vol. 39, no. 8, pp. 1662–1674, 2017.
- [21] R. Köhler, M. Hirsch, B. Mohler, B. Schölkopf, and S. Harmeling, "Recording and playback of camera shake: benchmarking blind deconvolution with a real-world database," in *Proceedings of the European Conference on Computer Vision*, pp. 27–40, Florence, Italy, October 2012.
- [22] M. Hirsch, C. J. Schuler, S. Harmeling, and B. Schölkopf, "Fast removal of non-uniform camera shake," in *Proceedings of the International Conference On Computer Vision*, pp. 463–470, Barcelona, Spain, November 2011.
- [23] D. Krishnan, T. Tay, and R. Fergus, "Blind deconvolution using a normalized sparsity measure," in *Proceedings of the IEEE Conference on Computer Vision and Pattern Recognition*, pp. 233–240, Colorado, CO, USA, July 2011.
- [24] O. Whyte, J. Sivic, and A. Zisserman, "Deblurring shaken and partially saturated images," in *Proceedings of the IEEE International Conference On Computer Vision Workshops (ICCV Workshops)*, pp. 745–752, Hyderabad, India, March 1992.
- [25] Y. Yan, W. Ren, Y. Guo, R. Wang, and X. Cao, "Image deblurring via extreme channels prior," in *Proceedings of the IEEE International Conference on Computer Vision and Pattern Recognition*, pp. 4003–4011, Honolulu, HI, USA, July 2017.